

LRPPRC regulates metastasis and glycolysis by modulating autophagy and the ROS/HIF1- α pathway in retinoblastoma

Kun Song,^{1,6} Bin Li,^{2,6} Ying-Ying Chen,³ Hua Wang,^{4,5} Kang-Cheng Liu,^{4,5} Wei Tan,^{4,5} and Jing Zou^{4,5}

¹Department of Gastrointestinal Surgery, Xiangya Hospital, Central South University, Changsha 410008, Hunan Province, China; ²National Clinical Research Center for Geriatric Disorders, Xiangya Hospital, Central South University, Changsha 410008, Hunan Province, China; ³Department of Ophthalmology, Hainan General Hospital, Haikou 570000, Hainan Province, China; ⁴Eye Center of Xiangya Hospital, Central South University, Changsha 410008, Hunan Province, China; ⁵Hunan Key Laboratory of Ophthalmology, No. 87 Xiangya Road, Kaifu District, Changsha 410008, Hunan Province, China

Retinoblastoma (RB) is the most common intraocular tumor among children. Leucine-rich pentatricopeptide repeat (PPR)-motif-containing protein (LRPPRC), a suppressor gene of autophagy, has been proven to play a regulatory role in tumor progression. However, little is known about functional roles and mechanisms of LRPPRC in RB progression. First, we performed a detailed analysis for RB and normal control. The expression of LRPPRC in the RB tissues was significantly higher than that in normal tissues. Moreover, LRPPRC suppression could repress tumor cell migration, invasion, glycolysis, and reactive oxygen species (ROS)/hypoxia-inducible factor-1 α (HIF1- α) pathway activation by mediating autophagy. Furthermore, overexpression of HIF1- α partially reversed the above changes induced by LRPPRC knockdown. The regulation of LRPPRC on tumor metastasis and glycolysis was also validated by a xenograft tumor assay. In summary, LRPPRC could regulate metastasis and glycolysis of RB by mediating autophagy suppression and further activating the ROS/HIF1- α pathway, and LRPPRC could be a promising prognostic biomarker for RB.

INTRODUCTION

Retinoblastoma (RB) is a major intraocular tumor in children, which is caused by inactivation of tumor-suppressor gene RB1 during the development of the retina. As a standard treatment, chemotherapy has been widely used in a variety of auxiliary local treatments to save the eyes and reduce the risk of secondary tumors. Systemic and local (ophthalmic artery/intravitreal) chemotherapy is the major therapeutic strategies of RB.^{1,2} However, there are limitations for the chemotherapy of RB, such as drug resistance and side effects.³ Therefore, further identification of biomarkers of RB progression will be helpful for developing new molecular prognostic indicators and novel treatment strategies.

It has been reported that leucine-rich pentatricopeptide repeat (PPR)-motif-containing protein (LRPPRC) was highly expressed in multiple tumors, including lung, gastric, colon, and breast cancers. Meanwhile, downregulation of LRPPRC can promote

apoptosis of lung adenocarcinoma and lymphoma cells and inhibit cell proliferation and invasion.^{4,5} However, functional roles of LRPPRC in the progression of RB remain unclear. Besides, previous studies showed that LRPPRC was an autophagy suppressor,⁶ which was upregulated in RB tissues in our pre-experiments. Nevertheless, whether LRPPRC regulates RB progression through inhibiting autophagy was still unknown.

Autophagy is induced by starvation or stress to form a double membrane vesicle (autophagosome).⁷⁻⁹ Then, autophagosome could capture intracellular substances and degrade with lysosomes.^{10,11} Autophagy is closely related to the regulation of invasion and metastasis of cancer cells, angiogenesis, or tumorigenesis, suggesting that induction of autophagy defects in tumor cells is a mechanism of tumor inhibition or tumor promotion.¹²⁻¹⁵ It is speculated that LRPPRC may inhibit autophagy and promote RB metastasis. It has also been reported that inhibition of autophagy can activate hypoxia-inducible factor-1 α (HIF1- α), and knockdown of HIF1- α can inhibit the survival and proliferation of tumor cells.¹⁶ In addition, inhibition of autophagy is related to the production of reactive oxygen species (ROS), which can promote tumor metastasis.^{17,18} As known, tumor cells mainly obtain energy through glycolysis to promote its growth and metastasis. Meanwhile, autophagy is closely implicated in tumor progression. In addition, glycolysis could also affect tumor progression.¹⁹ However, whether LRPPRC could modulate RB development and glycolysis through regulating autophagy needs to be further explored.

In this study, differential expression of LRPPRC in RB tissues and normal tissues was observed. In addition, LRPPRC might regulate

Received 7 January 2021; accepted 10 June 2021;
<https://doi.org/10.1016/j.omto.2021.06.009>.

⁶These authors contributed equally

Correspondence: Jing Zou, Eye Center of Xiangya Hospital, Central South University, and Hunan Key Laboratory of Ophthalmology, No. 87 Xiangya Road, Kaifu District, Changsha 410008, Hunan Province, China.

E-mail: jzou30@csu.edu.cn



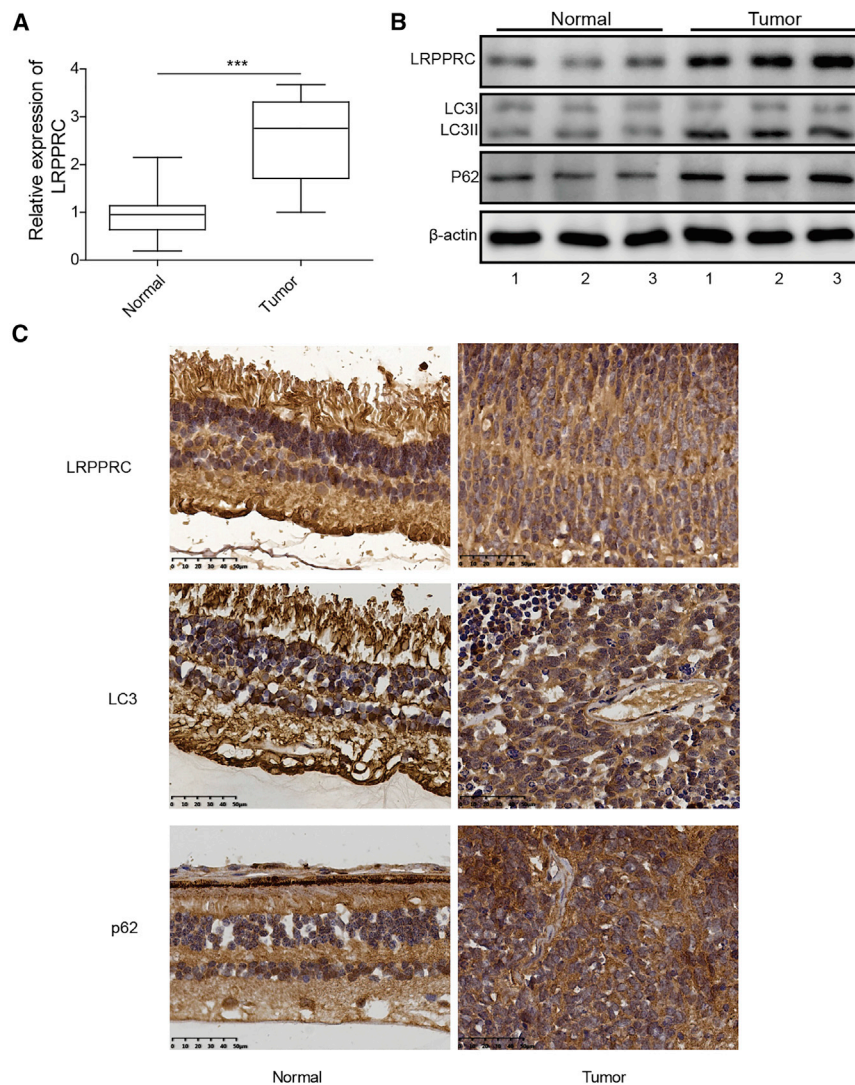


Figure 1. Differential expression of LRPPRC and autophagy-related molecules in RB

(A) Measurement of LRPPRC in the RB tissues and normal tissues beside the tumor by quantitative real-time PCR. The ratio between mean values of group experiment and group control were calculated, and relative expression was achieved. (B) Protein measurement of LRPPRC, LC3, and p62 by western blotting. (C) Measurement of LRPPRC, LC3, and p62 by immunohistochemical staining. * $p < 0.05$, ** $p < 0.01$, *** $p < 0.001$. Sample number: 30. LC3, light chain 3, including LC3 I and LC3 II. The adjacent normal tissues of RB patients were used as control.

western blotting and immunohistochemical staining (Figures 1B and 1C; Figure S1).

LRPPRC inhibited autophagy in RB cells

Next, the expression of LRPPRC in 4 different RB cell lines was detected, and the LRPPRC level was significantly higher than retinal pigment epithelial cells (Figure 2A). Y79 and WERI-Rb-1 with the highest expression of LRPPRC were applied for following experiments. To further clarify the relationship between LRPPRC and autophagy, lysosomal inhibitor (NH_4Cl) was used to intervene cells. Knockdown of LRPPRC was established by transfecting short hairpin (sh) LRPPRC in the Y79 and WERI-Rb-1 cell lines. Knockdown of LRPPRC by shLRPPRC significantly inhibited both mRNA and protein expression levels of LRPPRC, LC3, and p62 (Figures 2B–2D; Figure S2). However, after treatment with NH_4Cl , shLRPPRC remarkably increased the mRNA and protein expression of LC3 and P62 (Figures 2B–2D; Figure S2). The results

of LC3 were further validated by an immunofluorescence test (Figure 2E), and similar findings were observed.

metastasis and glycolysis of RB by mediating autophagy inhibition and further promoting ROS/HIF1- α pathway activation. This study is beneficial for better understanding of RB pathogenesis and may provide a novel idea about the therapeutic strategies of RB by targeting the LRPPRC/ROS/HIF1- α pathway.

RESULTS

Differential expression of LRPPRC and autophagy-related molecules in RB

The expression of LRPPRC in the RB tissues and normal tissues beside the tumor was first measured. The mRNA and protein expression of LRPPRC in the RB tissues was significantly higher than the normal group (Figures 1A and 1B; Figure S1). Light chain 3 (LC3) and p62 are two sensitive marker proteins of autophagy. Therefore, the levels of LC3 and p62 were also measured by western blot and immunohistochemical staining. The expression levels of LC3 and p62 were remarkably upregulated in tumor tissues measured by

of LC3 were further validated by an immunofluorescence test (Figure 2E), and similar findings were observed.

LRPPRC promoted cell migration, invasion, and glycolysis by inhibiting autophagy

The effects of LRPPRC on cell migration, invasion, and glycolysis in RB cells were further detected. Transfection with shLRPPRC markedly inhibited the migration and invasion of RB cells, but a combination with autophagy inhibitor (3-methyladenine [3-MA]) remarkably revised the influence of shLRPPRC treatment (Figures 3A and 3B). In addition, 3-MA showed inhibitory effects on cell migration and invasion (Figures S4A and S4B). Knockdown of LRPPRC significantly downregulated the protein expression of N-cadherin, vimentin, and Snail but upregulated the E-cadherin level. However, simultaneous treatment with 3-MA partly revised these trends (Figure 3C). Furthermore, LRPPRC repression remarkably inhibited glucose consumption and lactate production, but inhibition of autophagy could relieve

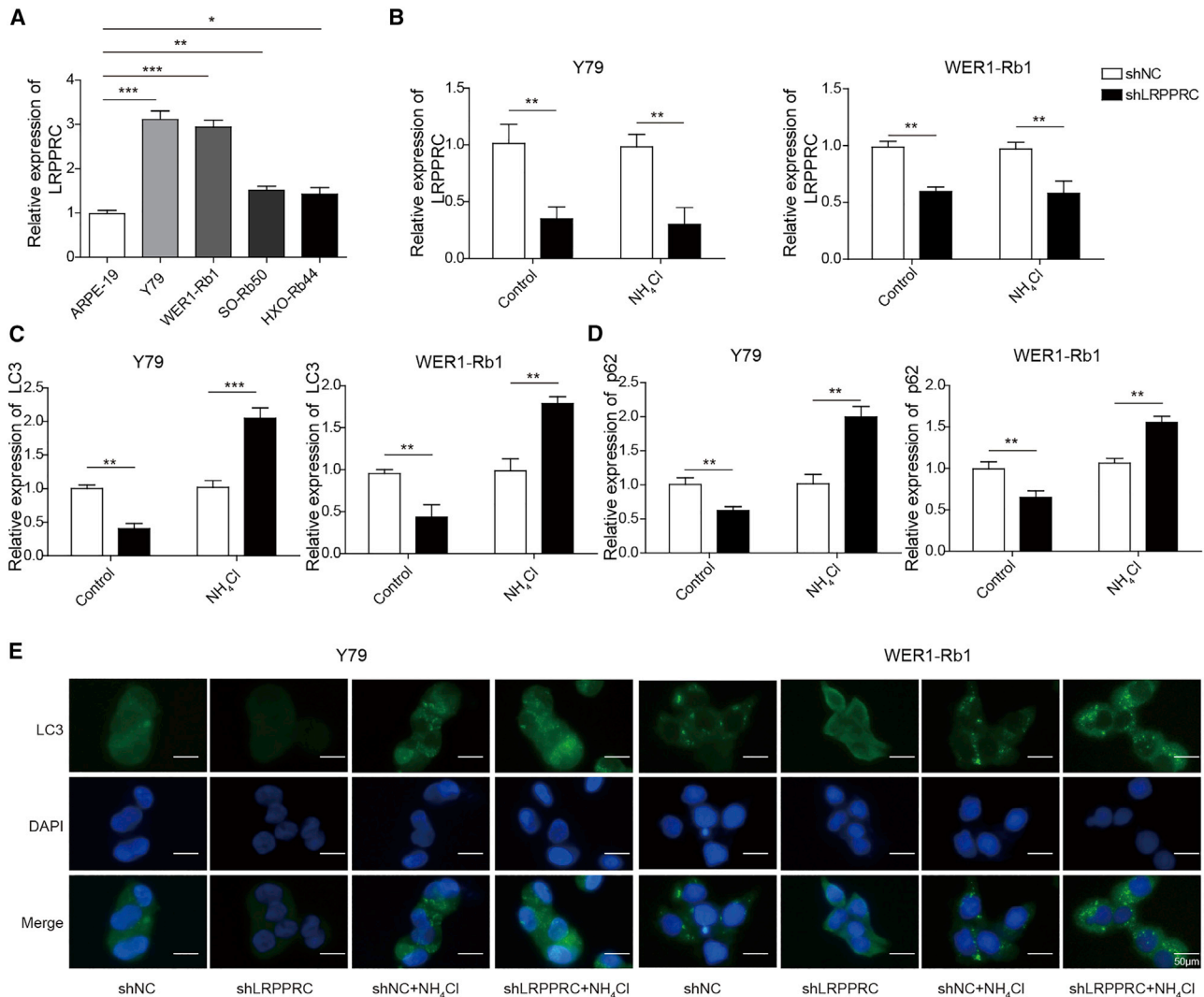


Figure 2. LRP-PRC inhibited autophagy in RB cells

(A) Expression of LRP-PRC in 4 different RB cell lines measured by quantitative real-time PCR. (B) Level of LRP-PRC in Y79 and WER1-Rb-1 cell lines examined by quantitative real-time PCR. (C) Measurement of LC3 in RB cell lines by quantitative real-time PCR. (D) Measurement of p62 in RB cells by quantitative real-time PCR. The ratio between mean values of group experiment and group control was calculated, and relative expression was achieved. (E) Measurement of LC3 in Y79 and WER1-Rb-1 cells by immunofluorescence. * $p < 0.05$, ** $p < 0.01$, *** $p < 0.001$. LC3, including LC3 I and LC3 II. Normal cell line: ARPE-19; RB cell lines: WER1-Rb1, Y79, SO-Rb50, and HXO-RB44.

these influence (Figure 3D). Meanwhile, transfection with shLRPPRC significantly suppressed the expression of glucose transporter 1 (GLUT1) and monocarboxylate transporter 1 (MCT1), which were partially blocked by the inhibition of autophagy (Figure 3E).

LRPPRC activated the ROS/HIF1- α pathway by inhibiting autophagy

To investigate the mechanism of LRP-PRC in regulating RB metastasis and glycolysis, the activation of ROS was assessed. Transfection with shLRPPRC and treatment with NH₄Cl significantly decreased intracellular ROS level as well as mitochondrial ROS level (Figures 4A and 4B). Then, we examined whether the activation of HIF1- α was related to the

increase of ROS in autophagy-deficient RB cells. After incubating with shLRPPRC and NH₄Cl, the protein level of HIF1- α was downregulated in comparison with the single treatment (Figure 4C).

Inhibition of the ROS/HIF1- α pathway partly reversed the functional role of LRP-PRC in RB cell migration, invasion, and glycolysis

Further, whether LRP-PRC promoted RB cell migration, invasion, and glycolysis via the activating ROS/HIF1- α pathway was investigated. After transfection, overexpression of HIF1- α could partially reverse the inhibition of cell migration and invasion in RB cells induced by LRP-PRC knockdown (Figures 5A and 5B). Meanwhile, NH₄Cl treatment could

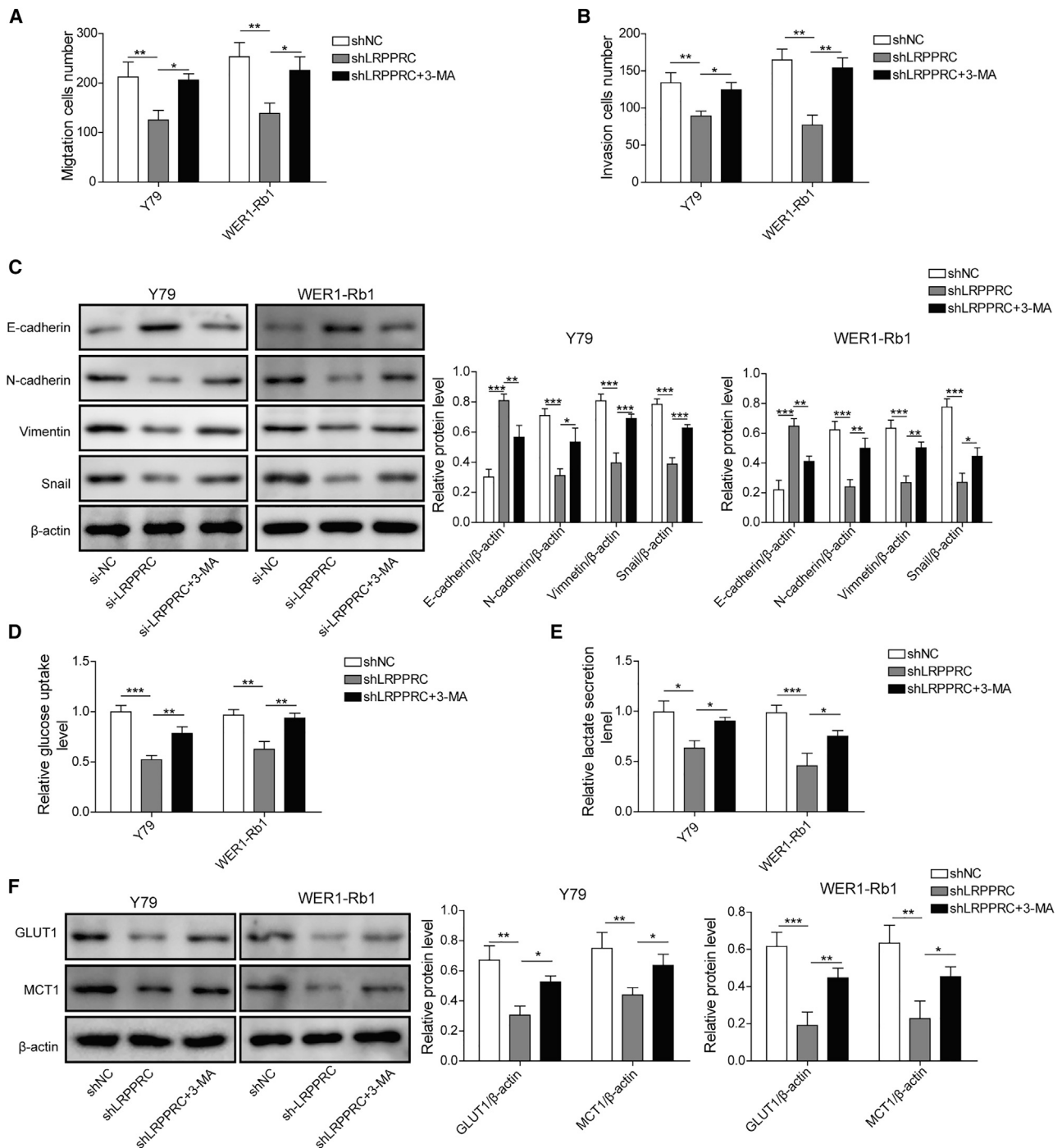


Figure 3. LRP13C promoted RB cell migration, invasion, and glycolysis by inhibiting autophagy

(A) Influence of LRP13C on cell migration of tumor cells assessed by Transwell assay. (B) Influence of LRP13C on cell invasion of tumor cells determined by Transwell assay. (C) Detection of LRP13C on EMT markers by western blotting. (D) Detection of glucose consumption. (E) Detection of lactate production. (F) Measurement of GLUT1 and MCT1 by western blotting. * $p < 0.05$, ** $p < 0.01$, *** $p < 0.001$. The ratio between mean values of target protein and β -actin was calculated, and relative expression was achieved.

suppress cell migration or invasion (Figures S3A and S3B). Additionally, overexpression of HIF1- α could also reverse the influence of shLRP13C on E-cadherin, N-cadherin, vimentin, and Snail expression

(Figure 5C). Besides, glucose consumption and lactate production decreased by LRP13C suppression were partly restrained under HIF1- α overexpression treatment (Figures 5D and 5E), which was

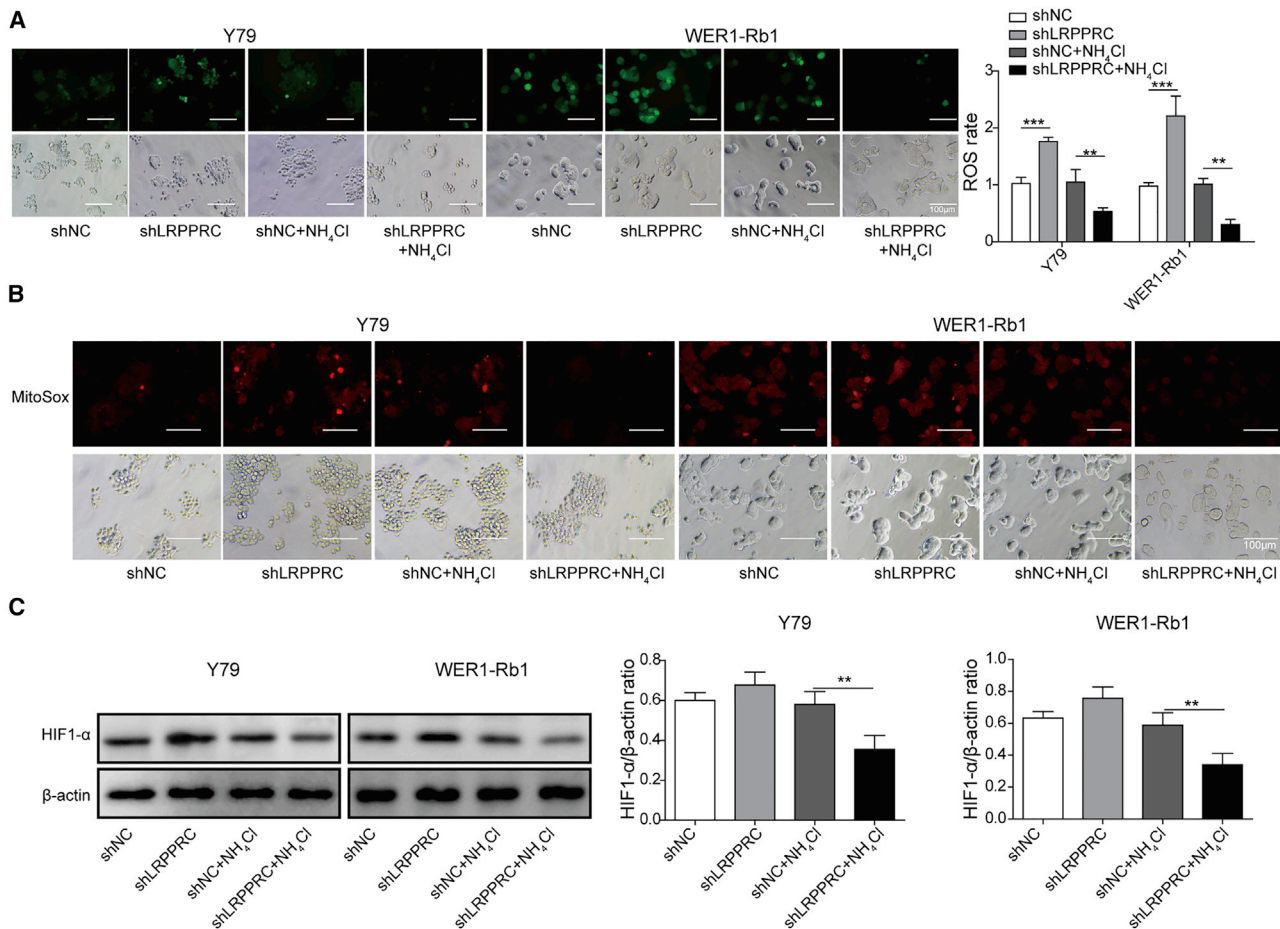


Figure 4. LRP-PRC activated the ROS/HIF1- α pathway by inhibiting autophagy

(A) Measurement of intracellular ROS level by DCF-DA. (B) Measurement of mitochondrial ROS level by MitoSOX Red. (C) The expression of HIF1- α measured by western blotting. * $p < 0.05$, ** $p < 0.01$, *** $p < 0.001$. The ratio between mean values of target protein and β -actin was calculated, and relative expression was achieved.

further confirmed by the results of GLUT1 and MCT1 protein levels (Figure 5F).

Verification of the regulation of LRP-PRC in RB metastasis and glycolysis *in vivo*

In vivo experiments were conducted to confirm our speculation that LRP-PRC may promote tumor metastasis and glycolysis by inhibiting autophagy and activating the ROS/HIF1- α pathway. Similar to the previous *in vitro* results, shLRPPRC significantly inhibited the tumor growth compared with the sh negative control (shNC)-treated group (Figures 6A and 6B). After removing tumors, tumor weights were examined, and the tumor weights in the shLRPPRC group were evidently lower than the control group (Figure 6C). Furthermore, knockdown of LRP-PRC suppressed the levels of LC3 and GLUT1 but promoted the expression of HIF1- α and E-cadherin (Figure 6D).

DISCUSSION

RB is the most common intraocular tumor in children, and it is mainly caused by inactivation of the RB suppressor gene. Eyeball

removal and laser treatment are major therapeutic strategies for RB. In addition, chemotherapy, commonly used for many types of tumors, has been shown to exert several adverse effects.²⁰ Therefore, better understanding of RB pathogenesis and searching for new and reliable markers could facilitate the new treatment for RB. In the present study, LRP-PRC could regulate RB cell migration, invasion, and glycolysis via mediating autophagy inhibition and ROS/HIF1- α activation.

Autophagy is a physiological response of cells to stress, and it is maintained at a low baseline level under normal circumstances. Several factors could activate autophagy, and autophagy can regulate the migration and invasive abilities in cancer cells. It has been proven that autophagy was involved in the progression and development of RB.^{21,22} LRP-PRC is known as an RNA-binding molecule, which is mainly located in the mitochondria. Previous study indicated that LRP-PRC could inhibit the activation of autophagy through promoting B cell lymphoma 2 (Bcl-2) stability under treatment of a lysosomal inhibitor (such as NH₄Cl).²³ Therefore, LRP-PRC may play a role in

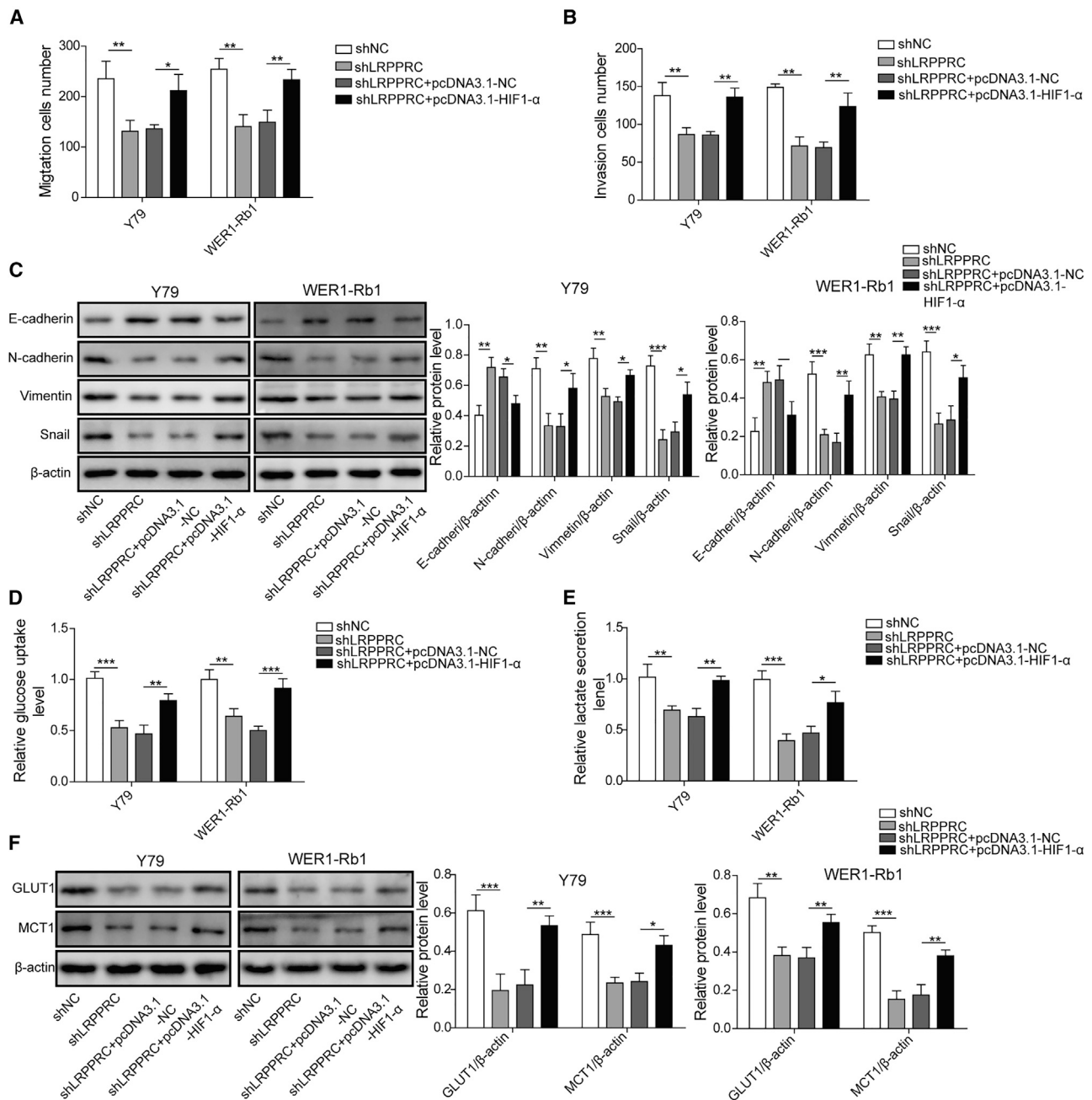


Figure 5. Inhibition of the ROS/HIF1- α pathway partly reversed the functional role of LRPPRC in RB cell migration, invasion, and glycolysis

(A) Influence of shLRPPRC and pcDNA3.1-HIF1- α on cell migration of tumor cells examined by Transwell assay. (B) Influence of shLRPPRC and pcDNA3.1-HIF1- α on cell invasion of tumor cells detected by Transwell assay. (C) Influence of shLRPPRC and pcDNA3.1-HIF1- α on EMT markers measured by western blotting. (D) Detection of glucose consumption after treatment with shLRPPRC and pcDNA3.1-HIF1- α . (E) Detection of lactate production after treatment with shLRPPRC and pcDNA3.1-HIF1- α . (F) Measurement of GLUT1 and MCT1 by western blotting after treatment with shLRPPRC and pcDNA3.1-HIF1- α . * $p < 0.05$, ** $p < 0.01$, *** $p < 0.001$. The ratio between mean values of target protein and β -actin was calculated, and relative expression was achieved.

cleaning up cellular debris and damaged mitochondria through inhibiting the initiation of autophagy. In addition, high expression of LRPPRC in several types of tumors, including lymphoma, colon, gastric, and lung cancers, was reported.²⁴ However, the role of

LRPPRC in RB and the specific regulatory mechanism remain unclear. In this study, LRPPRC was highly expressed in the RB tissues, and LRPPRC could suppress the autophagy in RB cells through regulating the expression of LC3 and p62. The remarkable inhibition of

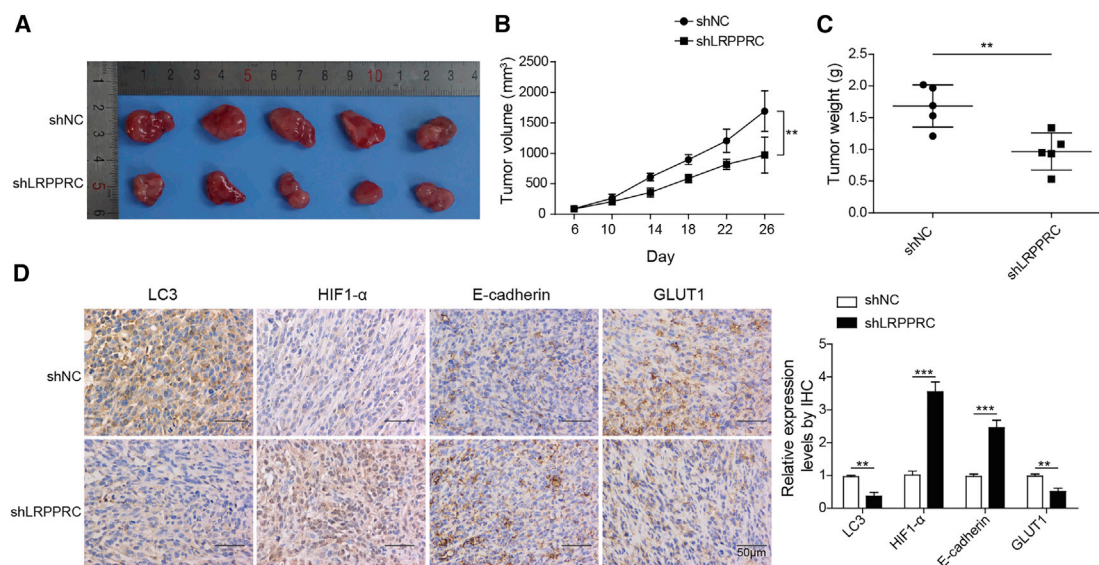


Figure 6. Verification of the regulation of LRPPRC on tumor metastasis and glycolysis *in vivo*

(A and B) Detection of xenograft tumor growth after nude mice after injection of Y79 cells transfected with shLRPPRC or shNC. (C) Analysis of tumor weight. (D) Investigation of LC3, GLUT1, HIF1- α , and E-cadherin expression in the tumor tissues by immunohistochemical staining. * $p < 0.05$, ** $p < 0.01$, *** $p < 0.001$. The ratio between mean values of group experiment and group control was calculated, and relative expression was achieved. LC3, including LC3 I and LC3 II.

LC3 and p62 by shLRPPRC could be significantly reversed by NH₄Cl (Figure 2). LC3 and p62 are associated with autophagosomal membranes that engulf cytoplasmic content for subsequent degradation.²⁵ Therefore, LRPPRC might inhibit the autophagy of RB cells through affecting autophagosomal membranes. These findings are in line with a previous study. In addition, the LC3 expression was downregulated by LRPPRC suppression, which may be due to the failure of intracellular proteins to degrade,²³ and the expression of LC3 upregulated by co-treatment with shLRPPRC and NH₄Cl confirmed this conjecture.

The cell migration, invasion, and glycolysis situation has been believed to be closely related with the metastasis of tumor. LRPPRC is believed to be involved in mitochondrial energy metabolism and glycolysis.²⁶ In addition, previous researches suggested that autophagy played a suppressive role in tumor metastasis.^{27,28} Meanwhile, negative regulation between autophagy and glycolysis has been identified in liver cancer.²⁹ In this study, the treatment with 3-MA, an autophagy inhibitor, could significantly reverse the suppression of tumor cell migration, invasion, and glycolysis induced by LRPPRC knockdown. These results indicate that LRPPRC might promote tumor cell migration, invasion, and glycolysis via suppressing autophagy in RB.

Previous reports indicated that suppression of autophagy could activate HIF1- α and ROS production.^{17,18} Meanwhile, LRPPRC was believed to be an inhibitor of autophagy.⁶ Therefore, LRPPRC might be a promoter of the ROS/HIF1- α pathway. The ROS pathway plays an important role in the dysfunction of mitochondrion, which is closely linked with the activation of autophagy.³⁰ In recent years, studies have shown that ROS can regulate the accumulation of

HIF1- α by promoting HIF1- α transcription and stabilizing protein stability.^{31–33} In addition, LRPPRC could regulate mitochondrial homeostasis through targeting HIF1- α .³⁴ Therefore, LRPPRC might regulate the ROS/HIF1- α pathway through affecting autophagy and further influence mitochondrion function. Knockdown of LRPPRC slightly upregulated the expression of ROS/HIF1- α , but treatment with the lysosomal inhibitor suppressed the level of ROS/HIF1- α , indicating LRPPRC could activate the ROS/HIF1- α pathway via suppressing autophagy. To further identify this finding, the overexpression vector of HIF1- α was constructed. Overexpression of HIF1- α could reverse the influence of LRPPRC inhibition on cell migration, invasion, epithelial-mesenchymal transition (EMT) markers (E-cadherin, N-cadherin, vimentin, and Snail) expression, glucose consumption, and lactate production. These results indicated that suppression of the ROS/HIF1- α pathway could reverse the effect of LRPPRC on tumor cell migration, invasion, and glycolysis. The *in vivo* study further confirmed the conclusion that LRPPRC could promote tumor metastasis and glycolysis through suppressing autophagy and activating the ROS/HIF1- α pathway. The specific mechanism of how LRPPRC inhibits autophagy and activates the ROS/HIF1- α signaling pathway is our future research direction. Additionally, knockdown of LRPPRC inhibited glucose consumption and lactate production, but inhibition of autophagy could relieve this influence. Therefore, although activation of glycolysis is known to decrease ROS, the inhibition of autophagy by LRPPRC could relieve the influence of glycolysis activation on ROS production. Meanwhile, LRPPRC might also affect the oxidative phosphorylation level of cells to exert effect on the ROS/HIF1- α pathway, which needs to be further investigated (Figure 7). Further, results in Figures S5A and S5B showed that suppression of LRPPRC downregulated Bcl-2 expression, providing

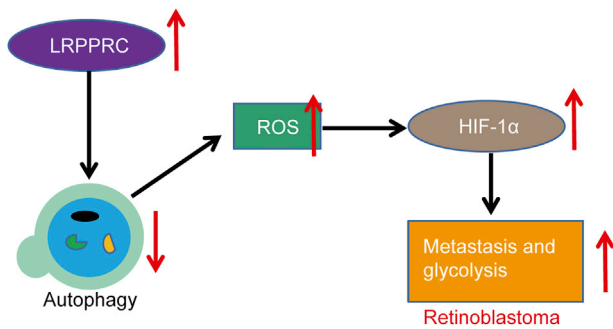


Figure 7. A schematic model of LRPPRC promoting tumor metastasis and glycolysis of RB via inhibition of autophagy and activation of ROS/HIF1- α pathway

evidence that LRPPRC may regulate autophagy via interacting with Bcl-2 in RB.²³

Conclusions

In summary, LRPPRC could promote tumor metastasis and glycolysis of RB, and the promotion function was achieved through inhibition of autophagy and activation of the ROS/HIF1- α pathway. Further, this study may help to speed up the evaluation of new prediction or therapeutic targets for RB.

MATERIALS AND METHODS

Clinical tissue samples

Thirty RB tissue samples and their paired adjacent normal tissues were collected from surgical resection between May 2014 and June 2018 at our hospital. All included RB patients did not undergo neoadjuvant chemotherapy before tissue collection. The histopathological diagnosis of all samples including RB tissue and adjacent normal tissue samples was respectively diagnosed by two experienced pathologists. Totally, 30 patients were included in this study. This study was approved by the Ethics Committee of Xiangya Hospital, Central South University (approval number: 202012226).

Cell culture

All cell lines (human retinal pigment epithelial cell line ARPE-19 [normal cells] and RB cell lines WERI-Rb1, Y79, SO-Rb50, and HXO-RB44 [tumor cell lines]) used in this study were purchased from American Type Culture Collection (ATCC; USA) and Cell Bank of Type Culture of Chinese Academy of Sciences (Shanghai, China). Cells were cultured using Roswell Park Memorial Institute (RPMI)-1640 or Dulbecco's modified Eagle's medium (DMEM) containing 10% fetal bovine serum (FBS) and then incubated in the incubator at 37°C with 5% CO₂. After passages, cells were applied for different experiments.

Cell transfection and treatment

Lentiviral vectors used for knockdown of LRPPRC (shLRPPRC) and overexpression of HIF1- α (pcDNA3.1-HIF1- α) were purchased from GeneChem (Shanghai, China). 2×10^4 cells were plated into a 12-well

and incubated for 24 h. Then, the virus was slowly melted on ice and added to the medium. Cell supernatant was discarded, and 1 mL of virus containing medium was added to each well. After incubation for 24 h, the transfection efficiency was observed by fluorescence microscopy. Then, the construction vectors for knockdown of LRPPRC and overexpression of HIF1- α were allowed for following experiments. Before measurement, 20 mM NH₄Cl (12 h) or 10 μ M 3-MA (6 h) was used to treat cells. 3-MA is the autophagy inhibitor, and NH₄Cl is the lysosomal inhibitor. NH₄Cl prevents the fusion of autophagy and lysosome by increasing the permeability of lysosome, and the process of autophagy is destroyed. 3-MA could inhibit autophagy by blocking autophagosome formation via the inhibition of type III phosphatidylinositol 3-kinases.

ROS measurement

For intracellular ROS measurement, dichlorofluorescein diacetate (DCF-DA) probe (10 μ M; Sigma, USA) was added and incubated at 37°C for 0.5 h. Then, cells were washed with serum-free medium to remove redundant DCF-DA. For mitochondrial ROS level detection, cells were treated with 5 μ M MitoSOX Red (Invitrogen, Carlsbad, CA, USA) for 30 min at 37°C. Finally, the ROS level was assessed using fluorescence microscopy.

Transwell assay

For cell-invasion detection, a 24-well Millicell chamber containing a Matrigel-coated membrane was used. In brief, RB cells were plated into the top chamber. The lower chamber was added with 1 mL medium containing 10% FBS. After 24 h, polyformaldehyde (4%) was added to lower chamber for fixation for 20 min. Then, 0.1% crystal violet was applied for staining. The invasion cell number was counted using an inverted microscope (BX53; Olympus, Tokyo, Japan). For cell migration assay, the operation is similar to the invasion assay except the Millicell chamber did not contain a Matrigel-coated membrane.

Glucose consumption and lactate production

Cells were transfected with shLRPPRC and then incubated 10 μ M 3-MA for 6 h or transfected with shLRPPRC and pcDNA3.1-HIF1- α for 24 h. After removing medium, glucose levels detected with a Glucose Assay Kit (BioVision, Milpitas, CA, USA) and lactate levels were measured with a Lactate Assay Kit (BioVision) following the methods provided by the manufacturer.

Western blot

Cells or tissues were lysed with lysis buffer (KeyGEN, Nanjing, China). Protein samples were loaded for 12% SDS-PAGE, and gels were transferred to the nitrocellulose membranes (Nanjing Jiancheng, China) and blocked with Tris-buffered saline-Tween 20 (TBST) for 1 h. Then, membranes were incubated with primary antibodies: LRPPRC (1:2,000; Abcam, Cambridge, MA, USA), LC3 (1:1,000; Abcam), p62 (1:1,000; Abcam), E-cadherin (1:2,000; Abcam), N-cadherin (1:1,000; Abcam), vimentin (1:2,000; Abcam), Snail (1:1,000; Abcam), GLUT1 (1:1,000; Abcam), MCT1 (1:2,000; Abcam), and HIF1- α (1:1,000; Abcam) at 4°C overnight. After washing, secondary

antibody (1:10,000; Abcam) was applied for 1 h incubation. After removing secondary antibody, membranes were visualized with the enhanced chemiluminescent detection system, and ImageJ software was used to analyze protein bands.

Quantitative real-time PCR

The total RNA from cells or tissues was separated using Trizol reagent (Takara, Japan), and reverse transcription was performed using a RevertAid First Strand cDNA Synthesis Kit (Thermo Scientific, Waltham, MA, USA). SYBR Premix Ex Taq II (Takara) was used for quantitative real-time PCR measurement on a CFX96 Touch Real-Time PCR Detection System (Bio-Rad, Hercules, CA, USA). The $2^{-\Delta\Delta CT}$ method was applied for analyzing the changes of target genes, which were normalized using glyceraldehyde 3-phosphate dehydrogenase (GAPDH) as the internal reference. The sequences of primers were listed as follows: LRPPRC (forward: 5'-ATCTGCAAGGCTT CAGTGGT-3', reverse: 5'-CATCAGCTCTTTGCCAGTCA-3'); LC3 (forward: 5'-GAAGTTCAGCCACCTGCCAC-3', reverse: 5'-TCTG AGGTGGAGGGTCAAGTC-3'); p62 (forward: 5'-GTACCAGGACA GCGAGAGGAA-3', reverse: 5'-CCCATGTTGCACGCCAAAC-3'); and GAPDH (forward: 5'-CCAGGTGGTCTCCTCTGA-3', reverse: 5'-GCTGTAGCCAAATCGTTGT-3').

Immunofluorescence assay

After treatment, cells in 6-well plates were washed with phosphate-buffered saline (PBS) and fixed by using 4% polyformaldehyde. Then, the primary antibody LC3 (1:200; Abcam) was allowed for cell incubation at 4°C overnight. Subsequently, cells were washed with PBS and incubated with goat anti-rabbit secondary antibody at a 1:1,000 dilution for 2 h. Lastly, DAPI (4',6-diamidino-2-phenylindole; Solarbio, Beijing, China) was used for nuclear staining, and images were visualized under a fluorescence microscope.

Immunohistochemical staining

4% formalin was used to fix tissues for 48 h. Then, tissues were embedded with optimal cutting temperature (OCT) compound (Sigma) and sectioned in 12 μ m thickness. After antigen repair, washing with PBS, and blocking with goat serum, primary antibody (LC3: 1:100, Abcam; p62: 1:250, Abcam; HIF1- α : 1:100, Abcam; E-cadherin: 1:500, Abcam; GLUT1: 1:250, Abcam) and secondary antibody were used to incubate tissues, respectively. Finally, 3,3'-diaminobenzidine (DAB) reagent was used to cultivate tissues, and sections were analyzed using a microscope.

Xenograft tumor assay

A xenograft tumor experiment was conducted in this study. Male nude mice were purchased from GemPharmatech (Nanjing, China) and randomly divided into 2 groups (5 mice/group). Y79 cells treated with shLRPPRC or shNC were subcutaneously injected into the back of mice. Tumor size was measured externally every 4 days. After 26 days, mice were sacrificed, and tumor weights were analyzed. Besides, immunohistochemical staining was performed on the embedded tumor tissues to assess LC3, HIF1- α , E-cadherin, and GLUT1 expression levels. All animal experiments were conducted ac-

ording to the national standard of the care and use of laboratory animals, and the study was approved by the Committee of Animal Research of Xiangya Hospital, Central South University (202004006).

Statistical analysis

Data were presented as mean \pm standard deviation (SD) and analyzed using GraphPad Prism 8 (GraphPad Software, La Jolla, CA, USA) via Student's t test (two groups) or one-way analysis of variance (ANOVA; multiple groups) as appropriate. $p < 0.05$ was believed to be statistical significance. All experiments were repeated three times.

SUPPLEMENTAL INFORMATION

Supplemental information can be found online at <https://doi.org/10.1016/j.omto.2021.06.009>.

ACKNOWLEDGMENTS

This study was approved by the Ethics Committee of Xiangya Hospital, Central South University. All animal experiments were conducted according to the national standard of the care and use of laboratory animals, and the study was approved by the Committee of Animal Research of Xiangya Hospital, Central South University. The study was supported by the National Natural Science Foundation of China (no. 81600713) and Young Researcher Grants of Xiangya Hospital (no. 2015Q05).

AUTHOR CONTRIBUTIONS

Conceptualization, J.Z.; methodology, J.Z.; investigation, B.L., K.S., and Y.-Y.C.; writing – original draft, K.S. and K.-C.L.; writing – review & editing, J.Z.; funding acquisition, K.S.; resources, H.W. and W.T.; supervision, H.W.

DECLARATION OF INTERESTS

The authors declare no competing interests.

REFERENCES

- Fan, X.Q. (2017). Pay attention to the application of the international intraocular retinoblastoma classification and sequential multiple modality treatment. *Zhonghua Yan Ke Za Zhi* 53, 561–565.
- Brink, A., Correa, Z.M., Geller, J., Abruzzo, T., and Augsburger, J.J. (2014). Managing the consequences of aggressive conservative treatment for refractory retinoblastoma with vitreous seeding. *Arq. Bras. Ophthalmol.* 77, 256–258.
- Geng, W., Ren, J., Shi, H., Qin, F., Xu, X., Xiao, S., Jiao, Y., and Wang, A. (2021). RPL41 sensitizes retinoblastoma cells to chemotherapeutic drugs via ATF4 degradation. *J. Cell. Physiol.* 236, 2214–2225.
- Cui, J., Wang, L., Ren, X., Zhang, Y., and Zhang, H. (2019). LRPPRC: A Multifunctional Protein Involved in Energy Metabolism and Human Disease. *Front. Physiol.* 10, 595.
- Zhang, H.Y., Ma, Y.D., Zhang, Y., Cui, J., and Wang, Z.M. (2017). Elevated levels of autophagy-related marker ULK1 and mitochondrion-associated autophagy inhibitor LRPPRC are associated with biochemical progression and overall survival after androgen deprivation therapy in patients with metastatic prostate cancer. *J. Clin. Pathol.* 70, 383–389.
- Zou, J., Li, W., Misra, A., Yue, F., Song, K., Chen, Q., Guo, G., Yi, J., Kimata, J.T., and Liu, L. (2015). The viral restriction factor tetherin prevents leucine-rich pentatricopeptide repeat-containing protein (LRPPRC) from association with beclin 1 and B-cell CLL/lymphoma 2 (Bcl-2) and enhances autophagy and mitophagy. *J. Biol. Chem.* 290, 7269–7279.

7. Qiang, L., Sample, A., Shea, C.R., Soltani, K., Macleod, K.F., and He, Y.Y. (2017). Autophagy gene ATG7 regulates ultraviolet radiation-induced inflammation and skin tumorigenesis. *Autophagy* 13, 2086–2103.
8. Wang, Z., Zhu, S., Zhang, G., and Liu, S. (2015). Inhibition of autophagy enhances the anticancer activity of bortezomib in B-cell acute lymphoblastic leukemia cells. *Am. J. Cancer Res.* 5, 639–650.
9. Yan, M.M., Ni, J.D., Song, D., Ding, M., and Huang, J. (2015). Interplay between unfolded protein response and autophagy promotes tumor drug resistance. *Oncol. Lett.* 10, 1959–1969.
10. He, L., Livingston, M.J., and Dong, Z. (2014). Autophagy in acute kidney injury and repair. *Nephron Clin. Pract.* 127, 56–60.
11. Peng, Y., Miao, H., Wu, S., Yang, W., Zhang, Y., Xie, G., Xie, X., Li, J., Shi, C., Ye, L., et al. (2016). ABHD5 interacts with BECN1 to regulate autophagy and tumorigenesis of colon cancer independent of PNPLA2. *Autophagy* 12, 2167–2182.
12. Jiang, M., Wei, Q., Dong, G., Komatsu, M., Su, Y., and Dong, Z. (2012). Autophagy in proximal tubules protects against acute kidney injury. *Kidney Int.* 82, 1271–1283.
13. Khezri, R., and Rusten, T.E. (2019). Autophagy and Tumorigenesis in *Drosophila*. *Adv. Exp. Med. Biol.* 1167, 113–127.
14. Huang, T., Song, X., Yang, Y., Wan, X., Alvarez, A.A., Sastry, N., Feng, H., Hu, B., and Cheng, S.Y. (2018). Autophagy and Hallmarks of Cancer. *Crit. Rev. Oncog.* 23, 247–267.
15. Berliocchi, L., Chiappini, C., Adornetto, A., Gentile, D., Cerri, S., Russo, R., Bagetta, G., and Corasaniti, M.T. (2018). Early LC3 lipidation induced by d-limonene does not rely on mTOR inhibition, ERK activation and ROS production and it is associated with reduced clonogenic capacity of SH-SY5Y neuroblastoma cells. *Phytomedicine* 40, 98–105.
16. Peng, X., Gong, F., Chen, Y., Jiang, Y., Liu, J., Yu, M., Zhang, S., Wang, M., Xiao, G., and Liao, H. (2014). Autophagy promotes paclitaxel resistance of cervical cancer cells: involvement of Warburg effect activated hypoxia-induced factor 1- α -mediated signaling. *Cell Death Dis.* 5, e1367.
17. Li, D., Xie, G., and Wang, W. (2012). Reactive oxygen species: the 2-edged sword of osteoarthritis. *Am. J. Med. Sci.* 344, 486–490.
18. Li, X., Liang, M., Jiang, J., He, R., Wang, M., Guo, X., Shen, M., and Qin, R. (2018). Combined inhibition of autophagy and Nrf2 signaling augments bortezomib-induced apoptosis by increasing ROS production and ER stress in pancreatic cancer cells. *Int. J. Biol. Sci.* 14, 1291–1305.
19. Li, W., Tanikawa, T., Kryczek, I., Xia, H., Li, G., Wu, K., Wei, S., Zhao, L., Vatan, L., Wen, B., et al. (2018). Aerobic Glycolysis Controls Myeloid-Derived Suppressor Cells and Tumor Immunity via a Specific CEBPB Isoform in Triple-Negative Breast Cancer. *Cell Metab.* 28, 87–103.e6.
20. Sultan, I., Hajja, Y., Nawaiseh, I., Mehyar, M., Deebajah, R., Jaradat, I., and Yousef, Y.A. (2016). Chemoreduction of Progressive Intraocular Retinoblastoma by Systemic Topotecan. *Ophthalmic Genet.* 37, 209–213.
21. Ciavarra, G., and Zacksenhaus, E. (2011). Direct and indirect effects of the pRb tumor suppressor on autophagy. *Autophagy* 7, 544–546.
22. Wang, C.Y., Xu, Z.B., Wang, J.P., Jiao, Y., and Zhang, B. (2017). Rb deficiency accelerates progression of carcinoma of the urinary bladder in vivo and in vitro through inhibiting autophagy and apoptosis. *Int. J. Oncol.* 50, 1221–1232.
23. Zou, J., Yue, F., Jiang, X., Li, W., Yi, J., and Liu, L. (2013). Mitochondrion-associated protein LRPPRC suppresses the initiation of basal levels of autophagy via enhancing Bcl-2 stability. *Biochem. J.* 454, 447–457.
24. Tian, T., Ikeda, J., Wang, Y., Mamat, S., Luo, W., Aozasa, K., and Morii, E. (2012). Role of leucine-rich pentatricopeptide repeat motif-containing protein (LRPPRC) for anti-apoptosis and tumorigenesis in cancers. *Eur. J. Cancer* 48, 2462–2473.
25. Schläfli, A.M.A.O., Adams, O., Galván, J.A., Gugger, M., Savic, S., Bubendorf, L., Schmid, R.A., Becker, K.F., Tschan, M.P., Langer, R., and Berezowska, S. (2016). Prognostic value of the autophagy markers LC3 and p62/SQSTM1 in early-stage non-small cell lung cancer. *Oncotarget* 7, 39544–39555.
26. Davison, E.J., Pennington, K., Hung, C.C., Peng, J., Rafiq, R., Ostareck-Lederer, A., Ostareck, D.H., Ardley, H.C., Banks, R.E., and Robinson, P.A. (2009). Proteomic analysis of increased Parkin expression and its interactants provides evidence for a role in modulation of mitochondrial function. *Proteomics* 9, 4284–4297.
27. Jia, L., Huang, S., Yin, X., Zan, Y., Guo, Y., and Han, L. (2018). Quercetin suppresses the mobility of breast cancer by suppressing glycolysis through Akt-mTOR pathway mediated autophagy induction. *Life Sci.* 208, 123–130.
28. Xia, X., Wang, L., Zhang, X., Wang, S., Lei, L., Cheng, L., Xu, Y., Sun, Y., Hang, B., Zhang, G., et al. (2018). Halofuginone-induced autophagy suppresses the migration and invasion of MCF-7 cells via regulation of STMN1 and p53. *J. Cell. Biochem.* 119, 4009–4020.
29. Jiao, L., Zhang, H.L., Li, D.D., Yang, K.L., Tang, J., Li, X., Ji, J., Yu, Y., Wu, R.Y., Ravichandran, S., et al. (2018). Regulation of glycolytic metabolism by autophagy in liver cancer involves selective autophagic degradation of HK2 (hexokinase 2). *Autophagy* 14, 671–684.
30. Green, P.D., Sharma, N.K., and Santos, J.H. (2019). Telomerase Impinges on the Cellular Response to Oxidative Stress Through Mitochondrial ROS-Mediated Regulation of Autophagy. *Int. J. Mol. Sci.* 20, 1509.
31. Galanis, A., Pappa, A., Giannakakis, A., Lanitis, E., Dangaj, D., and Sandaltzopoulos, R. (2008). Reactive oxygen species and HIF-1 signalling in cancer. *Cancer Lett.* 266, 12–20.
32. Koshikawa, N., Hayashi, J., Nakagawara, A., and Takenaga, K. (2009). Reactive oxygen species-generating mitochondrial DNA mutation up-regulates hypoxia-inducible factor-1 α gene transcription via phosphatidylinositol 3-kinase-Akt/protein kinase C/histone deacetylase pathway. *J. Biol. Chem.* 284, 33185–33194.
33. Shimojo, Y., Akimoto, M., Hisanaga, T., Tanaka, T., Tajima, Y., Honma, Y., and Takenaga, K. (2013). Attenuation of reactive oxygen species by antioxidants suppresses hypoxia-induced epithelial-mesenchymal transition and metastasis of pancreatic cancer cells. *Clin. Exp. Metastasis* 30, 143–154.
34. Zhang, Q., Cai, S., Guo, L., and Zhao, G. (2020). Propofol induces mitochondrial-associated protein LRPPRC and protects mitochondria against hypoxia in cardiac cells. *PLoS ONE* 15, e0238857.